The Henryk Niewodniczański
INSTITUTE OF NUCLEAR PHYSICS
Ul. Radzikowskiego 152, 31-342 Kraków, Poland.

www.ifj.edu.pl/reports/2000.html

Report No 1854/PH

Direct Energy Deposition in the Lateral Concrete Shielding of the TESLA Water Dump and the Rise of Shielding Temperature

D. Dworak and J. Loskiewicz

Abstract

A water beam dump for the TESLA electron-positron collider is being designed. Energy deposition and related power release in concrete shielding which is surrounding the dump are calculated using Monte-Carlo simulations. High values of the released power has been found which could result in a shield temperature increase of a few hundred centigrade and finally in a shield damage. Additional shielding by different materials (Fe, Al, C, and water) have been proposed for further shield designs. For all0 designed case energy deposited in the outer concrete shield is reduced about two orders of magnitude and kept near the limit needed.

Also is calculated the radiation field and its composition, fluences and energy spectra of the particles produced inside the dump and shielding.

Kraków, November 2000

Introduction

In the linear electron-positron collider TESLA, the electrons and positrons of each pulse of their beams should, after crossing the interaction zone, be dumped in a shielded underground dump. The mean power to be absorbed is 8 MW for 250 GeV beam energy and 12 MW for the 400 GeV case. According to Brinkmann et al [1] report there would be $2.04*10^{14}$ electrons/s in the beam for 250 GeV case and $2.8*10^{14}$ electrons/s for TDR case.

In the first design it was supposed to use a water dump consisting of water filled titanium cylinder of a diameter of 100 to 150 cm. The cylinder was supposed to be surrounded by 20-cm wide air gap and shielded by concrete walls one meter thick. The water dump was to be kept at the temperature of 80 ^{o} C through water circulation and outside cooling. The concrete shield was supposed not to be cooled and a temperature rise of only 10 to 20 degrees Celsius of the concrete was regarded as acceptable.

Calculations and Results

Using FLUKA code [2] we calculated the energy deposition in the concrete shielding. The calculations were performed for pure cylindrical geometry. The cross-section of the dump along the beam axis, as approximated in FLUKA, is shown in Fig.1. The concrete shielding was divided into fifty annular rings twenty centimeters thick and 100 cm wide forming five layers. These rings will be called concrete regions. There are ten regions in each layer. The calculations were performed using Leading Particle Biasing (LPB) approximation. The energy cut off was put at 10 keV for gamma rays and 100 keV for electrons. The distribution of deposited power along the beam axis in the innermost layer of concrete shield is shown in Fig. 2. The calculation was performed for a water dump of 50-cm radius. It can be seen that the maximum value of deposited power lays at the distance of 3 to 4 meters from the beam entry. The maximum value of power deposited in concrete is 15.7 kW per meter of annular ring for the water cylinder diameter of 100 cm and 5.8 kW/m for 150-cm diameter of the dump.

A very rough heat conduction calculation performed by A. Leuschner [3], shows that a 10 degrees K difference between successive 20-cm thick concrete layers is giving 115 W/m heat conduction. Thus the temperature rise caused by 15-kW/m power release would result in the concrete temperature higher than a few hundreds of degrees.

Therefore additional shielding between the water dump and considered concrete shield is required. Inside the water dump the particles are mainly electrons and gamma rays. This is shown in Table 1, where the fluences and radiation doses are enumerated in percentages of total fluence and dose. Therefore shielding material of high Z e.g. iron would be space efficient. The calculations were performed, however, for many shielding materials in order to give the designers an ample choice. The typical statistics was 700,000 beam particles. The calculations were performed for nine different materials or geometrical shielding arrangements:

1. Iron 20 cm thick and 30 cm air gap (Fe20)
2. Aluminum 60 cm thick and 30 cm air gap (Alu60)
3. Aluminum 75 cm and 200 cm air gap (Alu75)
4. Graphite 80 cm and 30 cm air gap (Gr80)
5. Iron 10 cm + 30 cm Al + air gap 30 cm (Fe10Al30a)

6. Iron 10 cm + 30 cm Al + air gap 100 cm (Fe10Al30b)
7. Iron 10 cm + 30 cm Al + air gap 200 cm (Fe10Al30c)
8. Iron 10 cm + 45 cm Al + air gap 200 cm (Fe10Al45)
9. Water shield 180 cm thick + air gap 30 cm (Wa180)

In above enumerated cases the additional shielding material surrounds directly the water dump vessel and the air gap separates this material from the 100-cm thick concrete shield.

Inside the water dump the radiation is mainly composed of electrons and gamma rays (Table 1). If we take as an example the first case (Fe20), then inside the iron shield there is an important neutron and charged hadron contribution as can be seen from the Table 2. If we move to the outer concrete shield, then the neutron component is dominating the fluence (Table 3). Thus, in the concrete layers the radiation is mainly neutrons and therefore important residual radiation from concrete is to be expected.

The values shown in Tables 1 to 3 are from the region of maximum of the deposited energy, i.e. at z = 2 – 3 m from the beam entry in the (Fe20) case. For the concrete shield (Table 3) region of the maximum energy deposition in the innermost 20-cm thick concrete layer (region 3 - see Fig. 1) has been used for fluences and doses calculation.

The spectra of neutrons, charged hadrons and gamma rays were also calculated for this case (Fe20). For the (Wa180) case were calculated spectra of neutrons and gamma rays in the first twenty centimeters of concrete. In Fig. 3 is shown the neutron spectrum obtained at the boundary dump water – titanium vessel (at the distance z = 3 to 4 meters from the beam entry point). An important 100 MeV peak (from intranuclear cascade) is visible. Fig. 4 shows the proton spectrum, which is quite symmetric around 150 MeV and Fig. 6 shows the π^- spectrum with a peak around 300 MeV whereas the π^+ spectrum is shown in Fig. 5. The gamma ray spectrum can be seen in Fig. 7. Here the modal energy lies around 150 keV but a long high-energy tail is visible.

The next figures show the spectra at the vessel – iron boundary. Fig. 8 shows the neutron spectrum and Fig. 9 the gamma ray spectrum. The relative decrease of 100 MeV neutron peak can be remarked. The spectra of particles incident on the concrete surface are shown in Fig. 10 (neutrons) and Fig.11 (gamma rays). In the neutron spectrum the further decrease of intranuclear cascade peak (100 MeV neutrons) can be remarked. The high-energy tail of gamma ray spectrum has disappeared in Fig. 11.

For the (Wa180) case only track length estimates are available. The neutron and gamma ray spectra in first twenty centimeters of concrete shield are shown in Fig. 12 and 13 respectively.

The results obtained for the maximum value of power deposited in concrete are summarized in the Table 4. Here the maximum power deposition values are ranging from 273 W/m to 94 W/m. Therefore they fall within the acceptable range. The longitudinal distribution of deposited power for (Fe10Al45) case and (Wa180) case are shown in Fig. 14 and 15. These distributions are more uniform than those for the no additional shielding case are. This means a more uniform temperature of the concrete and also that the temperature stresses in the concrete would be smaller. The (Fe10Al45) distribution is even more uniform than the one for (Wa180) case.

The radiation power is deposited in the whole of the concrete shield. The values of the power deposition in all concrete blocks are shown in Table 5 for (Fe10Al45) case and in Table 6 for (Wa180) case. It is evident that in all regions of concrete some temperature rise due the radiation power deposition is to be expected.

Thus, to assess fully the temperature of the inner concrete layer a fully-fledged finite element method calculation of the heat conduction will be necessary. It will be, however, necessary to limit the shield palette to two shield compositions, to keep the calculation time in sensible limits.
During these calculations arose the question of the correctness of the use of LPB in such calculations. In order to check the correctness of LPB, additional calculations were performed. A test run was submitted for 20-cm iron shield case, but the LPB method was not applied in the dump water region. Instead, to shorten the calculation time, higher energy cut-off was used – 5 MeV for gamma rays and 10 MeV for electrons and positrons. There were six jobs with 20,000 beam particles in each, which makes a total of 120,000 beam particles in the calculation. The comparison of these results with LPB calculations (in total 2,700,000 beam particles) is shown in the Table 7. Here are shown: energy deposition in GeV/m for NO LPB and with LPB calculations, the errors, and the differences between the values obtained with LPB and without LPB. The first ten concrete regions represent the innermost concrete layer and the regions numbered 11 to 20 are second layer blocks. It can be seen that:

1. Almost all LPB values are higher than the test run values – only values near the end of the layer where errors are high show opposite behavior
2. The difference at the maximum deposition amounts only to 5.0 or 4.4 % of the value, which is smaller than the accuracy needed
3. The position of the maximum has not shifted
4. The relative error of the NO LPB calculation is quite small at the maximum (0.5 %).

The first point has the meaning that the high cut-off values are slightly diminishing (by 5 t0 10 %) the energy deposition values. The small (< 5%) difference in the deposition values at the maximum means that no important bias is introduced in the results by the use of the LPB. This is corroborated by the fact that the position of the maximum energy deposition has not shifted. In addition we would like to stress that nearer to the beam axis, in the dump water and iron shield, the differences between LPB and NO LPB results (not shown) are smaller than the corresponding statistical errors. As the use of LPB is giving a factor of more than two hundred in the speed of the calculation (if we compare the time to calculate the history of one beam particle), we will keep its use in further calculations.

Conclusions

Because of high value of energy deposition in the concrete, the no intermediate shield version of the dump design is to be modified. An additional shield near the water dump is to be introduced composed of an iron-aluminum sandwich or in the form of a great water tank. Other shield compositions were enumerated also.
It is evident that in all regions of concrete some temperature rise due the radiation energy deposition is to be expected. Thus, to assess fully the temperature of the inner concrete layer, a fully-fledged finite element method calculation of the heat conduction will be necessary. Also calculations of residual radioactivity should be done in near future. It will be, however, necessary to limit the shield palette to two shield compositions, in order to keep the calculation time in sensible limits.

References

1. R.Brinkmann, G. Materlik, J. Rossbach, A. Wagner (editors),
   Conceptual Design of a 500 GeV e^+ e^- Linear Collider with integrated X-ray Laser Facility, DESY 1997 – 048
2. A. Fasso, A. Ferrari, P. Sala, J. Ranft,
   FLUKA 99 Users Manual
3. A. Leuschner,
   Private communication

Table 1
Particle fluences and doses in the WATER of the dump

Particles	Fluence	Dose
Neutrons (E< 20 MeV)	**0**	0
Neutrons (E> 20 MeV)	**0**	**0**
All neutrons	**0**	**0**
Pions	**0**	**1**
Protons & pions	**0**	1
Gamma's	**95**	**31**
Electrons (+ & -)	**5**	**68**
E – M cascade	**100**	**99**

Table 2
In IRON shield

Particles	Fluence	Dose
Neutrons (E< 20 MeV)	**10**	**39**
Neutrons (E > 20 MeV)	**1**	**10**
All Neutrons	**11**	**49**
Pions	**0**	**12**
Protons &pions	**0**	**16**
Gamma's	**87**	**11**
Electrons (+ & -)	**2**	**24**
E – M Cascade	**89**	**35**

Table 3
In CONCRETE shield

Particles	Fluence	Dose
Neutrons (E < 20 MeV)	**60**	**57**
Neutrons (E > 20 MeV)	**2**	**21**
All Neutrons	**62**	**78**
Pions	**0**	**8**
Protons & pions	**0**	**13**
Gamma's	**37**	**3**
Electrons (+ & -)	**1**	**5**
E – M Cascade	**38**	**9**

Table 4
Maximum power deposition behind different shields

Shield composition	Air gap (cm)	Region of maximum	Deposed power (W/m)
Fe 20 cm	**30**	**3**	**247.3**
Al 60 cm	**30**	**3**	**210.2**
Al 75 cm	**200**	**4**	**99.1**
Graphite 80 cm	**30**	**4**	**273.0**
Fe 10 cm + Al 30 cm	**30**	**4**	**227.5**
Fe 10 cm + Al 30 cm	**100**	**4**	**189.4**
Fe 10 cm + Al 30 cm	**200**	**4**	**137.0**
Fe 10 cm + Al 45 cm	**200**	**4**	**94.1**
Water 180 cm	**30**	**4**	**106.0**

Map of power released in the 50 regions of the concrete shield (*)

Table 5
Case: Fe 10 cm + Al 45 cm

	Column									
	1	2	3	4	5	6	7	8	9	10
Regions	**Released power (W/m)**									
41-50	**3.6**	**3.0**	**6.3**	**7.0**	**7.5**	**6.1**	**4.0**	**3.8**	**1.9**	**0.8**
31-40	**4.1**	**7.5**	**13.0**	**12.4**	**12.4**	**10.5**	**8.9**	**4.9**	**2.8**	**2.4**
21-30	**7.0**	**14.9**	**20.1**	**23.7**	**23.2**	**19.4**	**13.1**	**9.3**	**6.9**	**3.3**
11-20	**16.0**	**29.2**	**45.7**	**49.7**	**45.4**	**34.4**	**24.5**	**15.9**	**10.6**	**8.1**
1-10	**36.0**	**65.9**	**85.8**	**94.1**	**88.5**	**64.2**	**47.7**	**30.7**	**19.4**	**14.3**

Table 6
Case: Water 180 cm

Regions	Released power (W/m)									
41-50	**2.0**	**3.7**	**7.0**	**5.4**	**6.3**	**3.8**	**5.3**	**3.3**	**1.1**	**0.6**
31-40	**3.7**	**6.7**	**10.0**	**13.4**	**12.9**	**6.3**	**7.4**	**4.3**	**1.6**	**1.0**
21-30	**4.8**	**14.7**	**20.1**	**28.2**	**19.0**	**14.9**	**9.2**	**7.1**	**4.2**	**1.8**
11-20	**16.5**	**26.8**	**37.9**	**47.7**	**43.2**	**37.2**	**18.3**	**11.6**	**5.6**	**3.2**
1-10	**27.6**	**49.4**	**85.6**	**106.**	**94.1**	**77.4**	**48.9**	**25.6**	**13.1**	**8.5**

(*) Position of each figure (released power) in the tables 5 and 6 corresponds "one-to-one" to position of the concrete region in the concrete shield (see Fig. 1). For instance, power released in region 34 is included in the fourth column of the second row (Regions 31-40) of the tables (12.4 W/m in case of table 5, and 13.4 W/m in case of table 6). Each concrete region is always 1 m long and 20 cm thick , but of variable radius in in different layers.

Table 7

Comparison of calculation results in concrete with LPB and NO LPB Case Fe 20 cm

Region of concrete	I NO LPB (GeV/m)	σ(I) (%)	II LPB (GeV/m)	σ(II) (%)	Difference (II-I)/II (%)
1	$1.394*10^{-3}$	1.1	$1.475*10^{-3}$	4.2	5.5
2	$4.659*10^{-3}$	0.7	$6.154*10^{-3}$	4.4	9.5
3	$7.449*10^{-3}$	0.5	$7.841*10^{-3}$	3.3	5.0
4	$7.063*10^{-3}$	0.5	$7.388*10^{-3}$	3.3	4.4
5	$4.675*10^{-3}$	1.4	$5.025*10^{-3}$	3.3	7.0
6	$2.465*10^{-3}$	1.3	$2.832*10^{-3}$	5.4	12.9
7	$1.172*10^{-3}$	3.2	$1.298*10^{-3}$	6.1	9.7
8	$5.025*10^{-4}$	4.3	$4.727*10^{-4}$	4.3	-6.3
9	$2.238*10^{-4}$	5.6	$2.113*10^{-4}$	4.9	-5.9
10	$9.144*10^{-5}$	9.4	$9.612*10^{-5}$	8.1	4.9
11	$6.465*10^{-4}$	1.4	$8.161*10^{-4}$	7.4	20.9
12	$2.185*10^{-3}$	1.2	$2.246*10^{-3}$	4.4	2.7
13	$3.598*10^{-3}$	1.0	$3.963*10^{-3}$	2.6	9.2
14	$3.518*10^{-3}$	1.0	$3.536*10^{-3}$	2.8	0.5
15	$2.429*10^{-3}$	1.3	$2.583*10^{-3}$	2.1	6.0
16	$1.362*10^{-3}$	1.7	$1.437*10^{-3}$	6.3	5.0
17	$6.359*10^{-4}$	1.7	$6.698*10^{-4}$	5.6	5.1
18	$2.653*10^{-4}$	4.2	$3.784*10^{-4}$	20.3	29.9
19	$1.105*10^{-4}$	4.4	$1.469*10^{-4}$	6.2	24.8
20	$4.766*10^{-5}$	16.1	$4.696*10^{-5}$	8.0	-1.5

Remark:
σ means the relative stndard deviation: SD/mean value * 100%

Water beam dump (cylindrical), cross-section through the beam axis

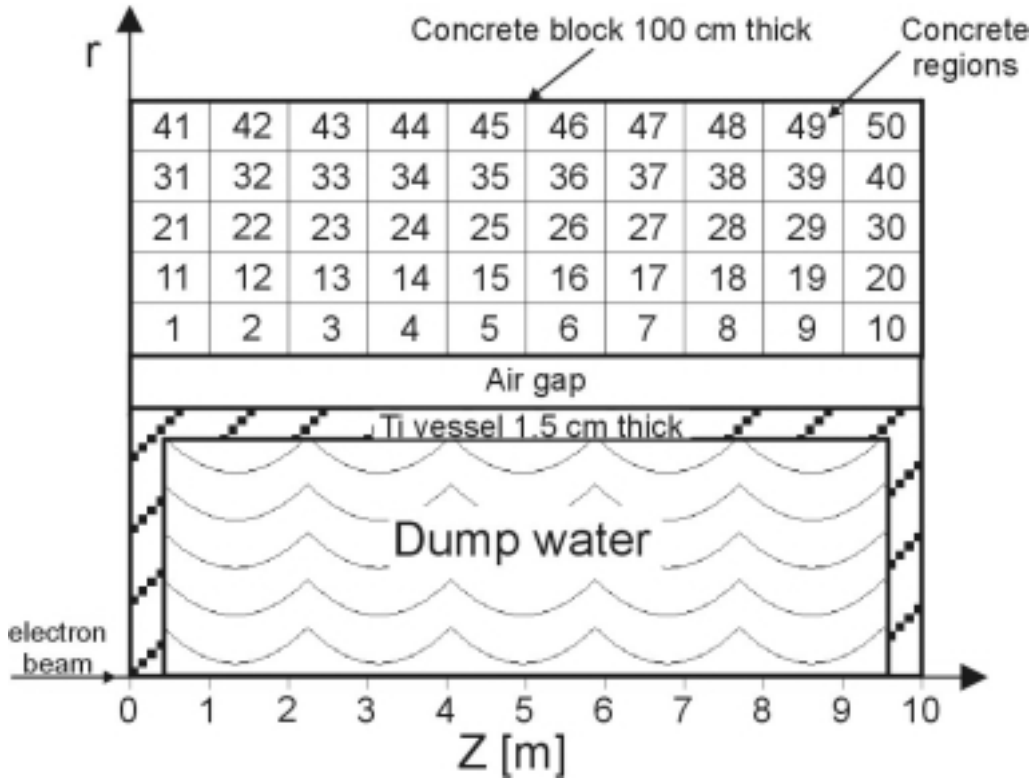

Fig. 1.

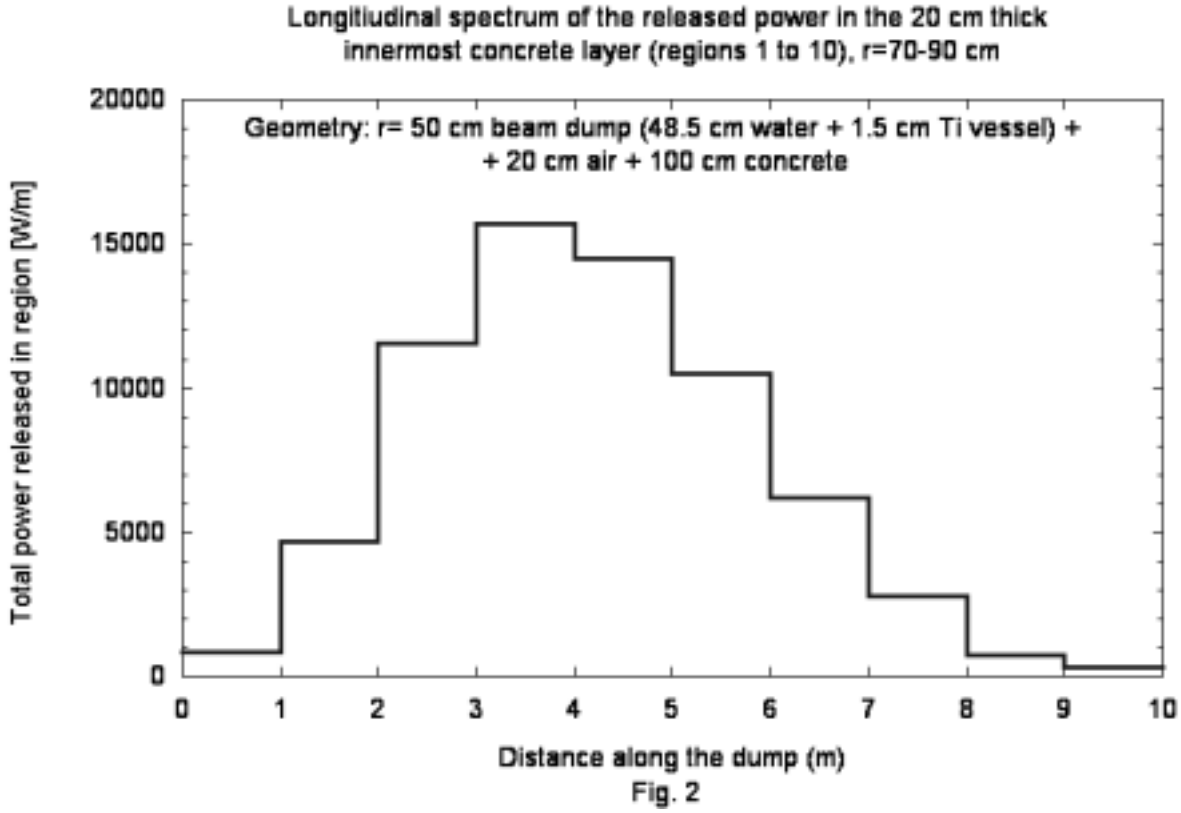

Fig. 2

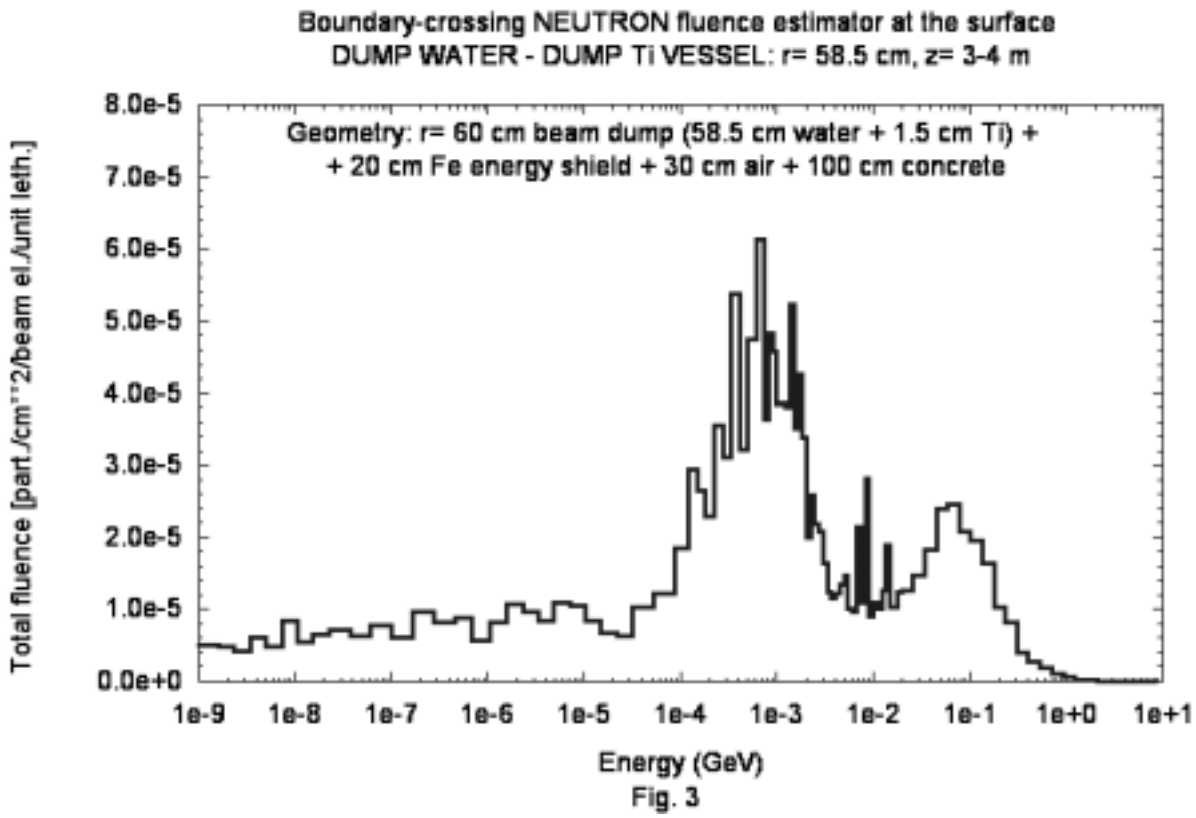
Boundary-crossing NEUTRON fluence estimator at the surface
DUMP WATER - DUMP Ti VESSEL: r= 58.5 cm, z= 3-4 m
Geometry: r= 60 cm beam dump (58.5 cm water + 1.5 cm Ti) +
+ 20 cm Fe energy shield + 30 cm air + 100 cm concrete
Total fluence [part./cm**2/beam el./unit leth.]
8.0e-5
7.0e-5
6.0e-5
5.0e-5
4.0e-5
3.0e-5
2.0e-5
1.0e-5
0.0e+0
1e-9
1e-8
1e-7
1e-6
1e-5
1e-4
1e-3
1e-2
1e-1
1e+0
1e+1
Energy (GeV)

Fig. 3

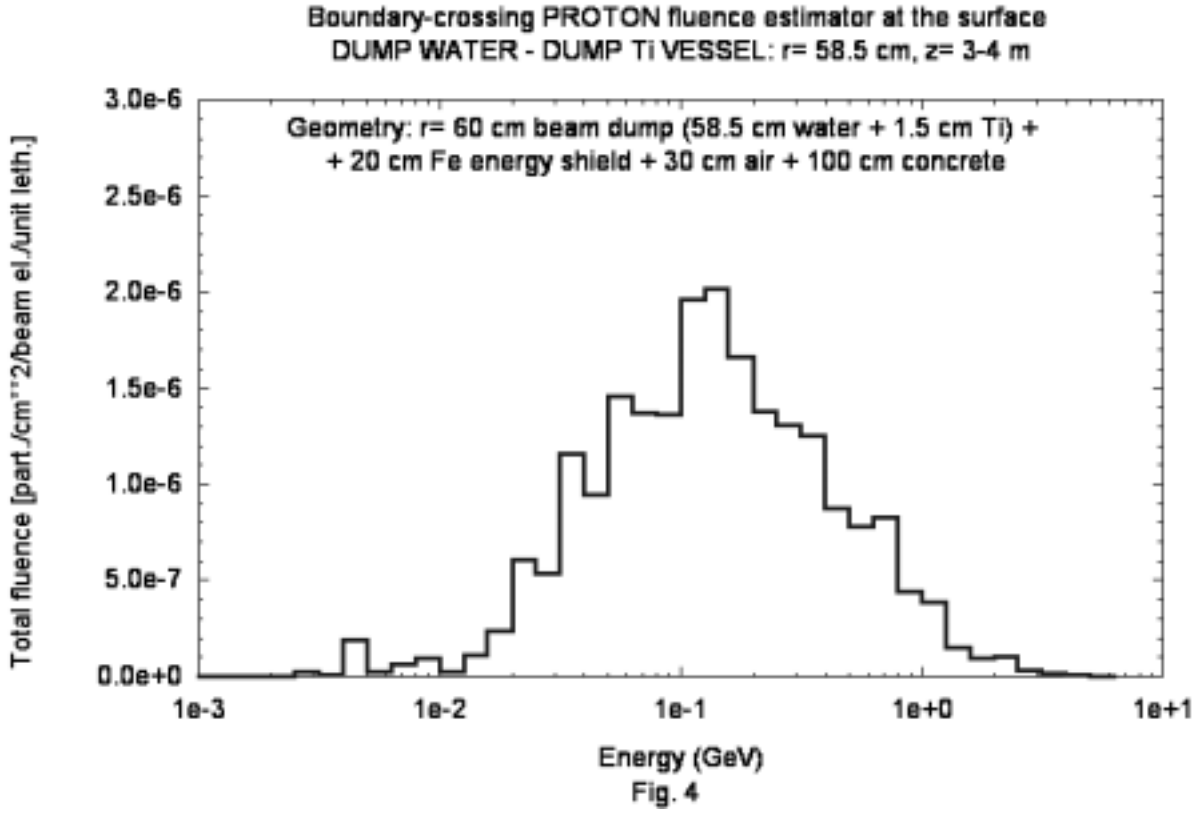
Boundary-crossing PROTON fluence estimator at the surface
DUMP WATER - DUMP Ti VESSEL: r= 58.5 cm, z= 3-4 m
Geometry: r= 60 cm beam dump (58.5 cm water + 1.5 cm Ti) +
+ 20 cm Fe energy shield + 30 cm air + 100 cm concrete
Total fluence [part./cm**2/beam el./unit leth.]
3.0e-6
2.5e-6
2.0e-6
1.5e-6
1.0e-6
5.0e-7
0.0e+0
1e-3
1e-2
1e-1
1e+0
1e+1
Energy (GeV)

Fig. 4

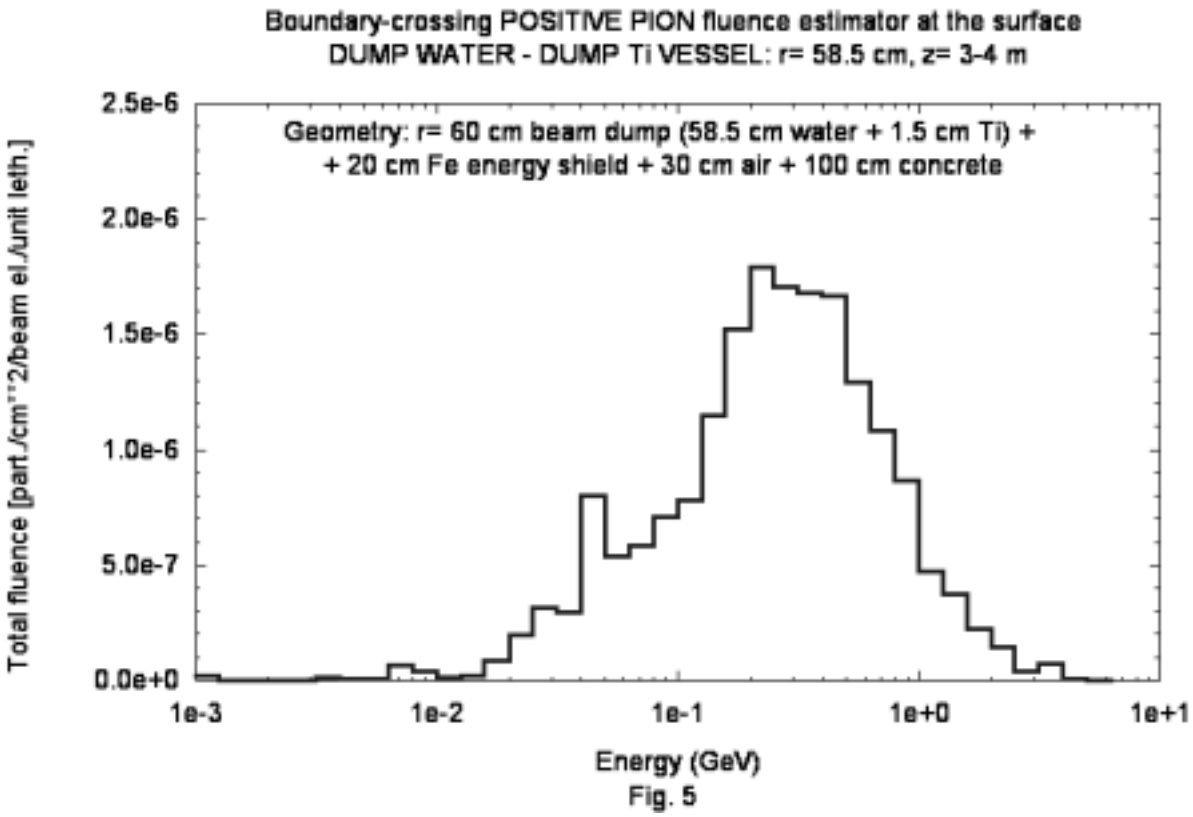
Boundary-crossing POSITIVE PION fluence estimator at the surface
DUMP WATER - DUMP Ti VESSEL: r= 58.5 cm, z= 3-4 m
Geometry: r= 60 cm beam dump (58.5 cm water + 1.5 cm Ti) +
+ 20 cm Fe energy shield + 30 cm air + 100 cm concrete
Total fluence [part./cm**2/beam el./unit leth.]
2.5e-6
2.0e-6
1.5e-6
1.0e-6
5.0e-7
0.0e+0
1e-3
1e-2
1e-1
1e+0
1e+1
Energy (GeV)
Fig. 5

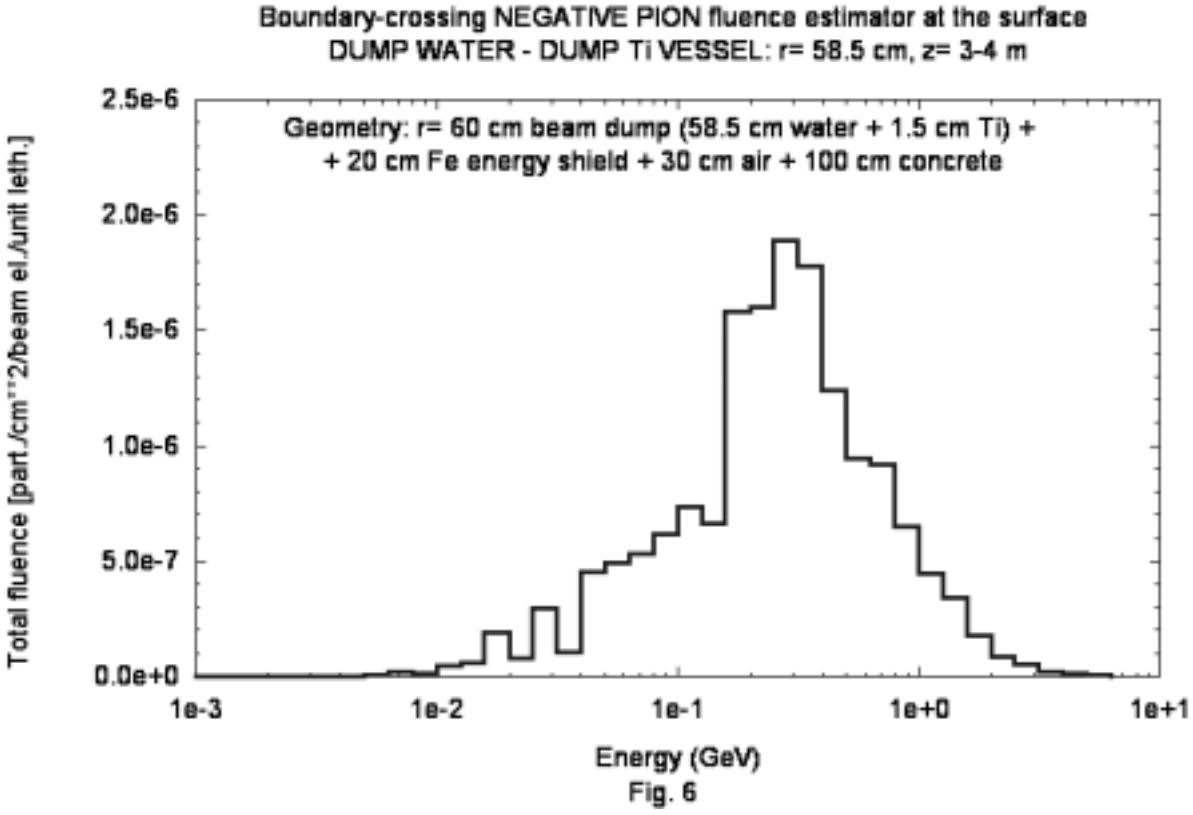
Boundary-crossing NEGATIVE PION fluence estimator at the surface
DUMP WATER - DUMP Ti VESSEL: r= 58.5 cm, z= 3-4 m
Geometry: r= 60 cm beam dump (58.5 cm water + 1.5 cm Ti) +
+ 20 cm Fe energy shield + 30 cm air + 100 cm concrete
Total fluence [part./cm**2/beam el./unit leth.]
2.5e-6
2.0e-6
1.5e-6
1.0e-6
5.0e-7
0.0e+0
1e-3
1e-2
1e-1
1e+0
1e+1
Energy (GeV)
Fig. 6

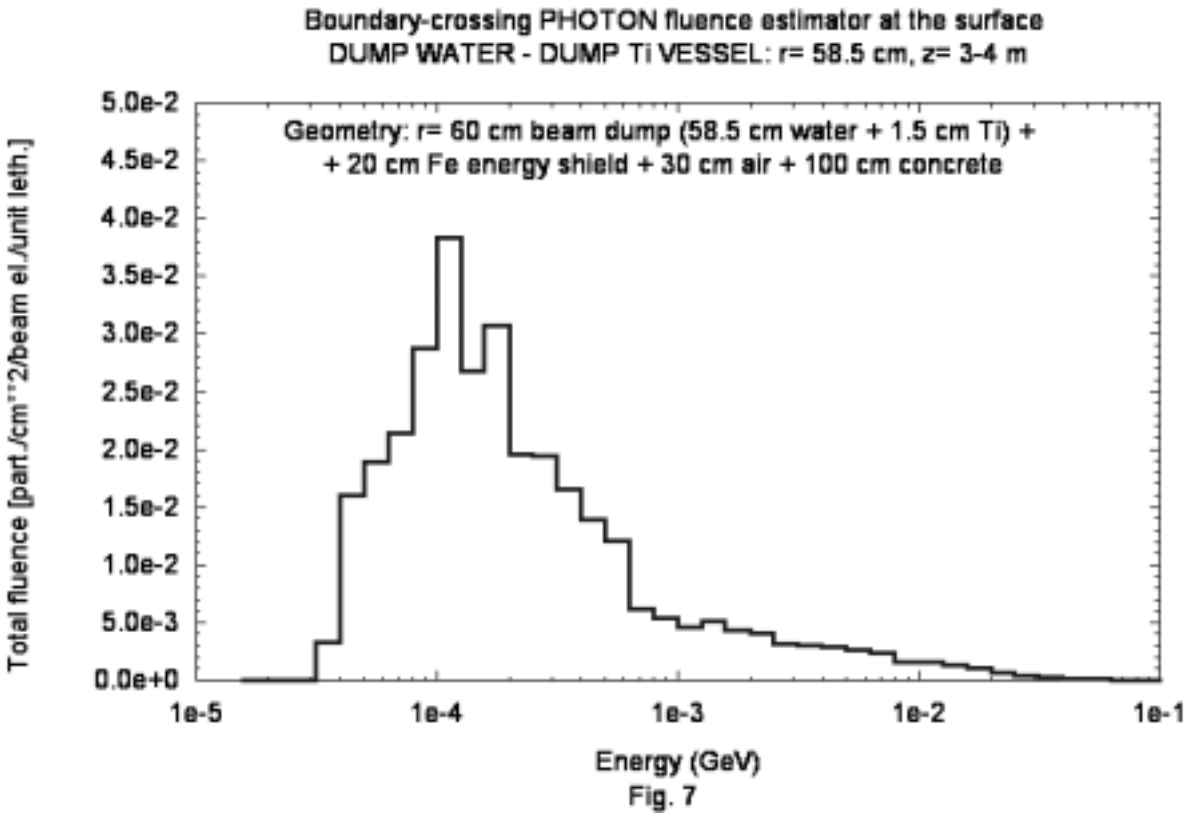
Boundary-crossing PHOTON fluence estimator at the surface
DUMP WATER - DUMP Ti VESSEL: r= 58.5 cm, z= 3-4 m
Geometry: r= 60 cm beam dump (58.5 cm water + 1.5 cm Ti) +
+ 20 cm Fe energy shield + 30 cm air + 100 cm concrete
Total fluence [part./cm**2/beam el./unit leth.]
5.0e-2
4.5e-2
4.0e-2
3.5e-2
3.0e-2
2.5e-2
2.0e-2
1.5e-2
1.0e-2
5.0e-3
0.0e+0
1e-5
1e-4
1e-3
1e-2
1e-1
Energy (GeV)
Fig. 7

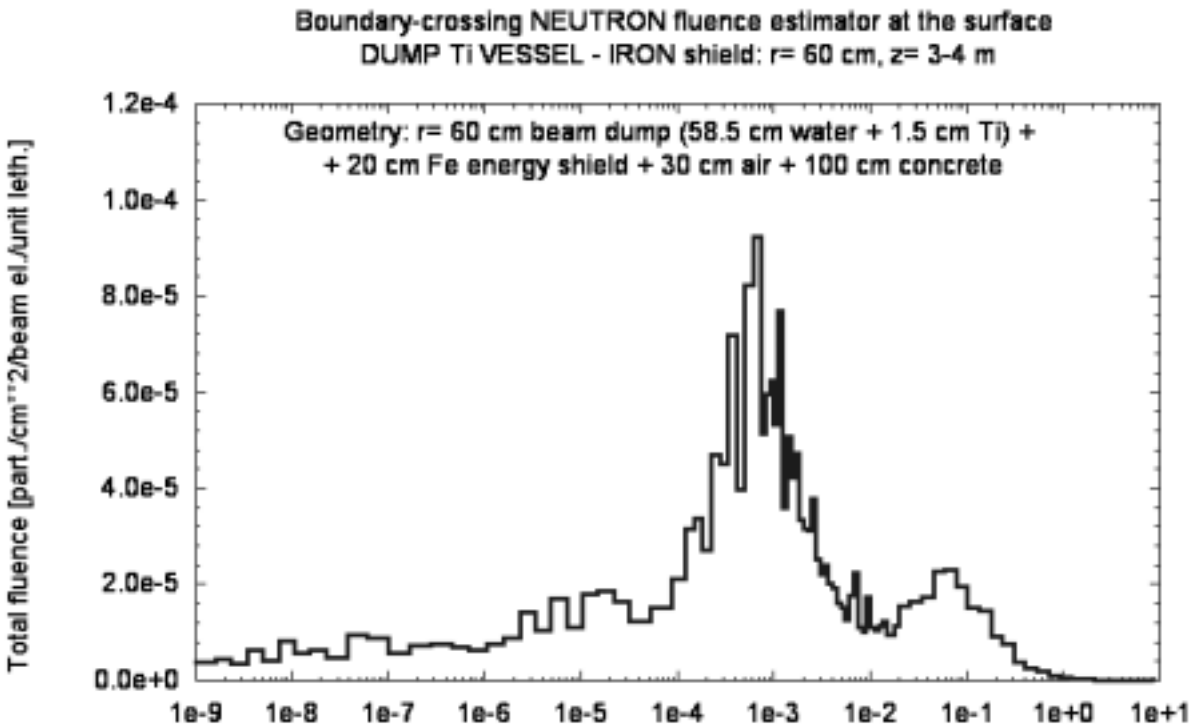
Boundary-crossing NEUTRON fluence estimator at the surface
DUMP Ti VESSEL - IRON shield: r= 60 cm, z= 3-4 m
Geometry: r= 60 cm beam dump (58.5 cm water + 1.5 cm Ti) +
+ 20 cm Fe energy shield + 30 cm air + 100 cm concrete
Total fluence [part./cm**2/beam el./unit leth.]
1.2e-4
1.0e-4
8.0e-5
6.0e-5
4.0e-5
2.0e-5
0.0e+0
1e-9
1e-8
1e-7
1e-6
1e-5
1e-4
1e-3
1e-2
1e-1
1e+0
1e+1
Energy (GeV)
Fig. 8

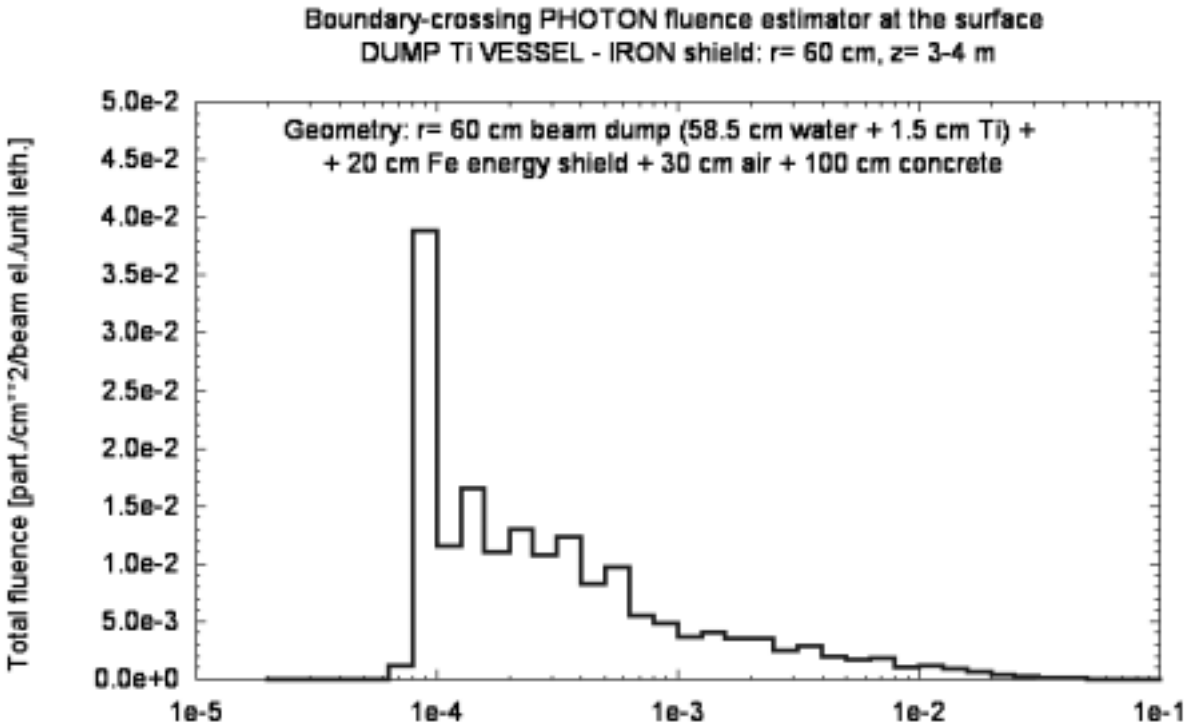
Boundary-crossing PHOTON fluence estimator at the surface
DUMP Ti VESSEL - IRON shield: r= 60 cm, z= 3-4 m
Geometry: r= 60 cm beam dump (58.5 cm water + 1.5 cm Ti) +
+ 20 cm Fe energy shield + 30 cm air + 100 cm concrete
Total fluence [part./cm**2/beam el./unit leth.]
5.0e-2
4.5e-2
4.0e-2
3.5e-2
3.0e-2
2.5e-2
2.0e-2
1.5e-2
1.0e-2
5.0e-3
0.0e+0
1e-5
1e-4
1e-3
1e-2
1e-1
Energy (GeV)
Fig. 9

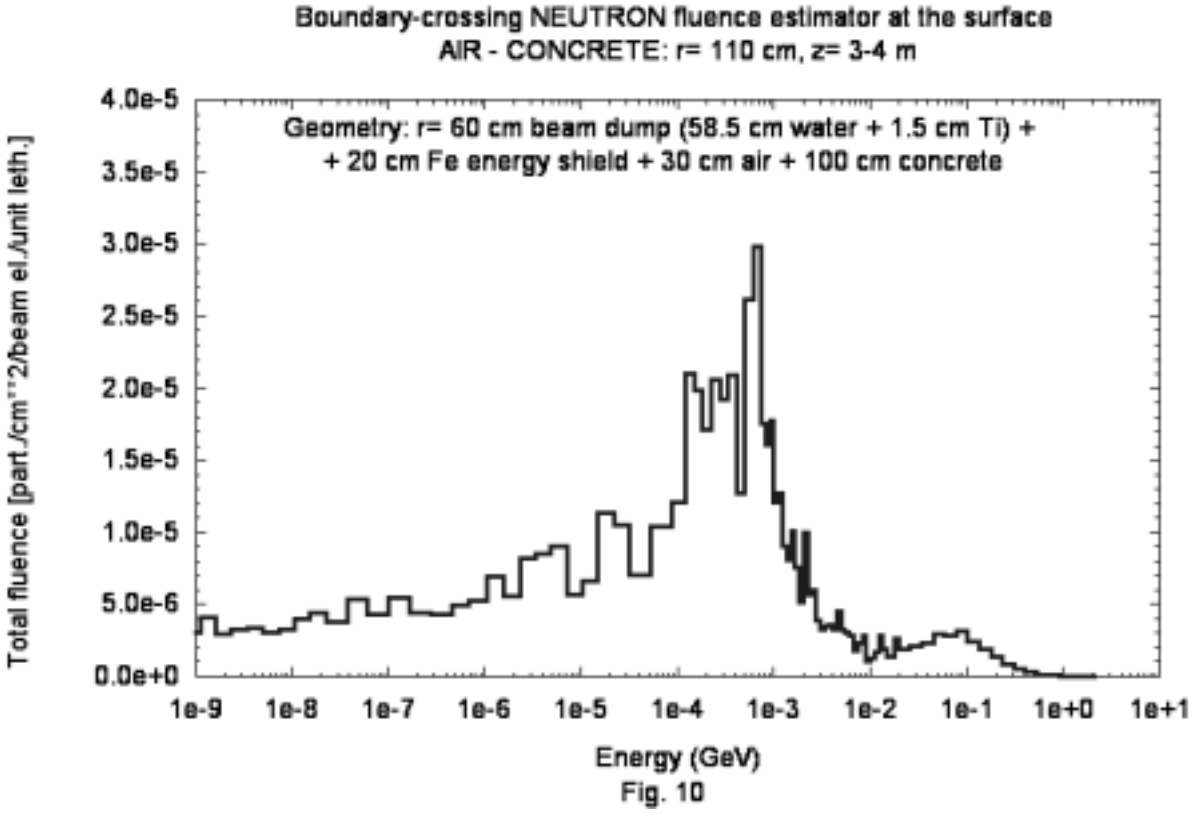
Boundary-crossing NEUTRON fluence estimator at the surface
AIR - CONCRETE: r= 110 cm, z= 3-4 m
Geometry: r= 60 cm beam dump (58.5 cm water + 1.5 cm Ti) +
+ 20 cm Fe energy shield + 30 cm air + 100 cm concrete
Total fluence [part./cm**2/beam el./unit leth.]
4.0e-5
3.5e-5
3.0e-5
2.5e-5
2.0e-5
1.5e-5
1.0e-5
5.0e-6
0.0e+0
1e-9
1e-8
1e-7
1e-6
1e-5
1e-4
1e-3
1e-2
1e-1
1e+0
1e+1
Energy (GeV)
Fig. 10

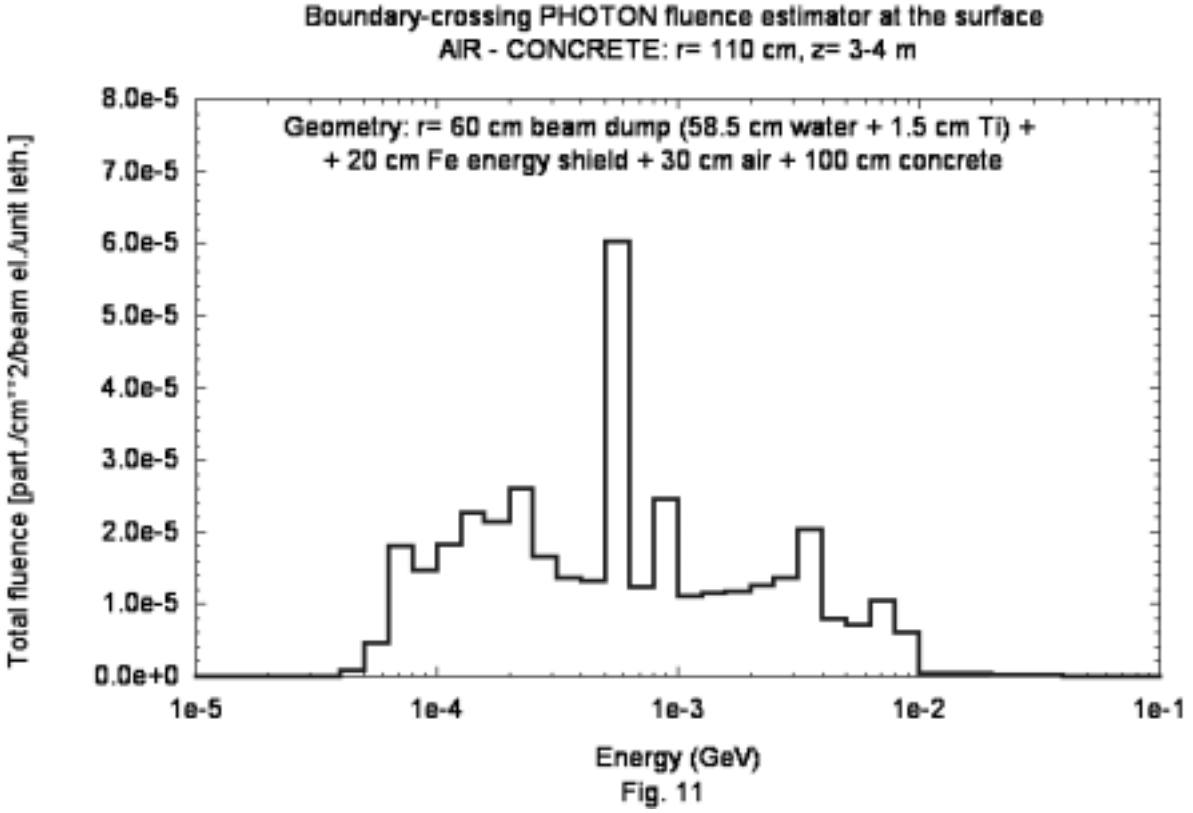
Boundary-crossing PHOTON fluence estimator at the surface
AIR - CONCRETE: r= 110 cm, z= 3-4 m
Geometry: r= 60 cm beam dump (58.5 cm water + 1.5 cm Ti) +
+ 20 cm Fe energy shield + 30 cm air + 100 cm concrete
Total fluence [part./cm**2/beam el./unit leth.]
8.0e-5
7.0e-5
6.0e-5
5.0e-5
4.0e-5
3.0e-5
2.0e-5
1.0e-5
0.0e+0
1e-5
1e-4
1e-3
1e-2
1e-1
Energy (GeV)
Fig. 11

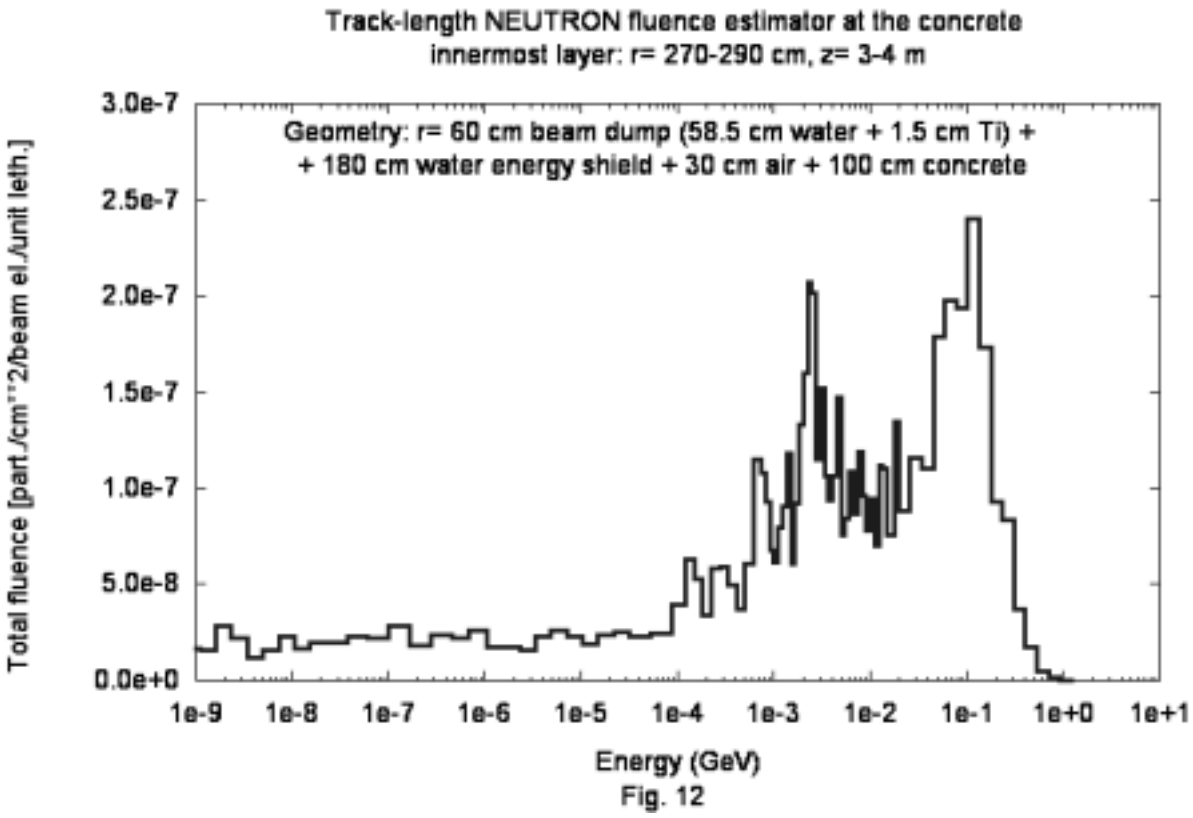
Track-length NEUTRON fluence estimator at the concrete
innermost layer: r= 270-290 cm, z= 3-4 m
Geometry: r= 60 cm beam dump (58.5 cm water + 1.5 cm Ti) +
+ 180 cm water energy shield + 30 cm air + 100 cm concrete
Total fluence [part./cm**2/beam el./unit leth.]
3.0e-7
2.5e-7
2.0e-7
1.5e-7
1.0e-7
5.0e-8
0.0e+0
1e-9
1e-8
1e-7
1e-6
1e-5
1e-4
1e-3
1e-2
1e-1
1e+0
1e+1
Energy (GeV)
Fig. 12

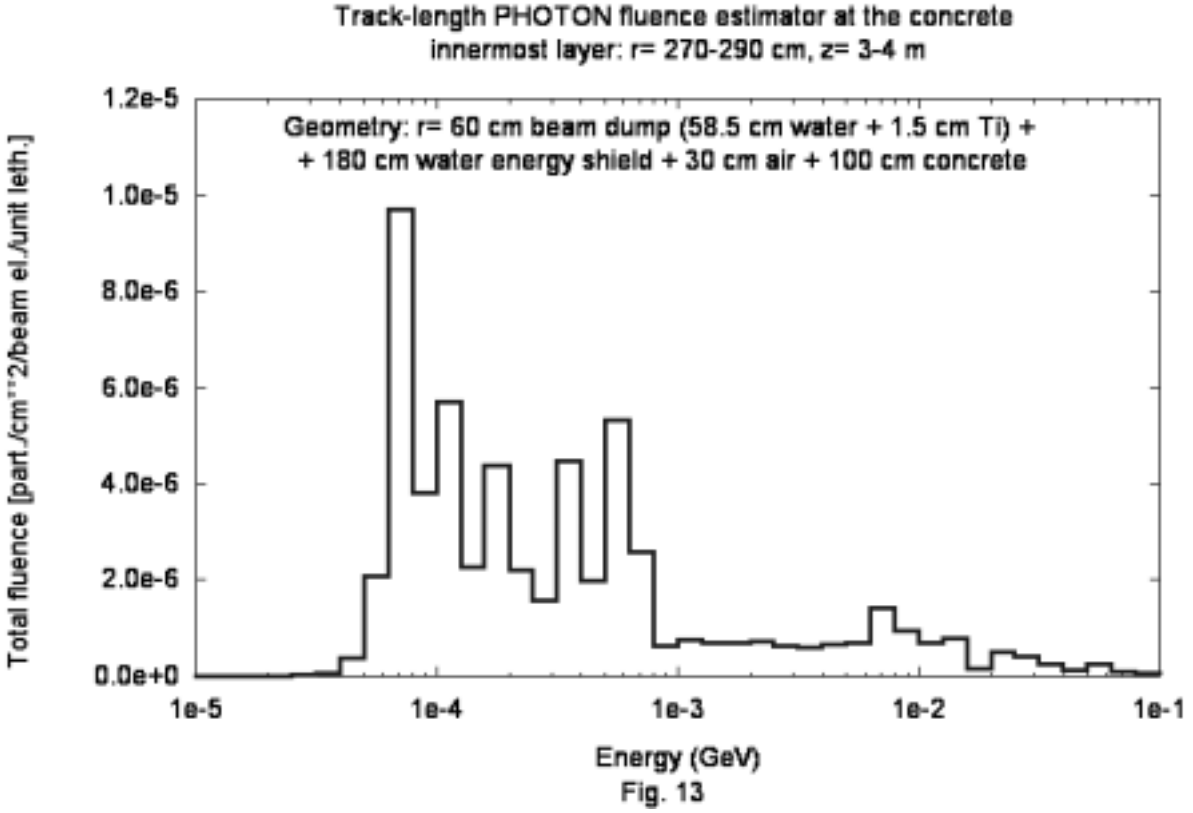
Track-length PHOTON fluence estimator at the concrete
innermost layer: r= 270-290 cm, z= 3-4 m
Geometry: r= 60 cm beam dump (58.5 cm water + 1.5 cm Ti) +
+ 180 cm water energy shield + 30 cm air + 100 cm concrete
Total fluence [part./cm**2/beam el./unit leth.]
1.2e-5
1.0e-5
8.0e-6
6.0e-6
4.0e-6
2.0e-6
0.0e+0
1e-5
1e-4
1e-3
1e-2
1e-1
Energy (GeV)
Fig. 13

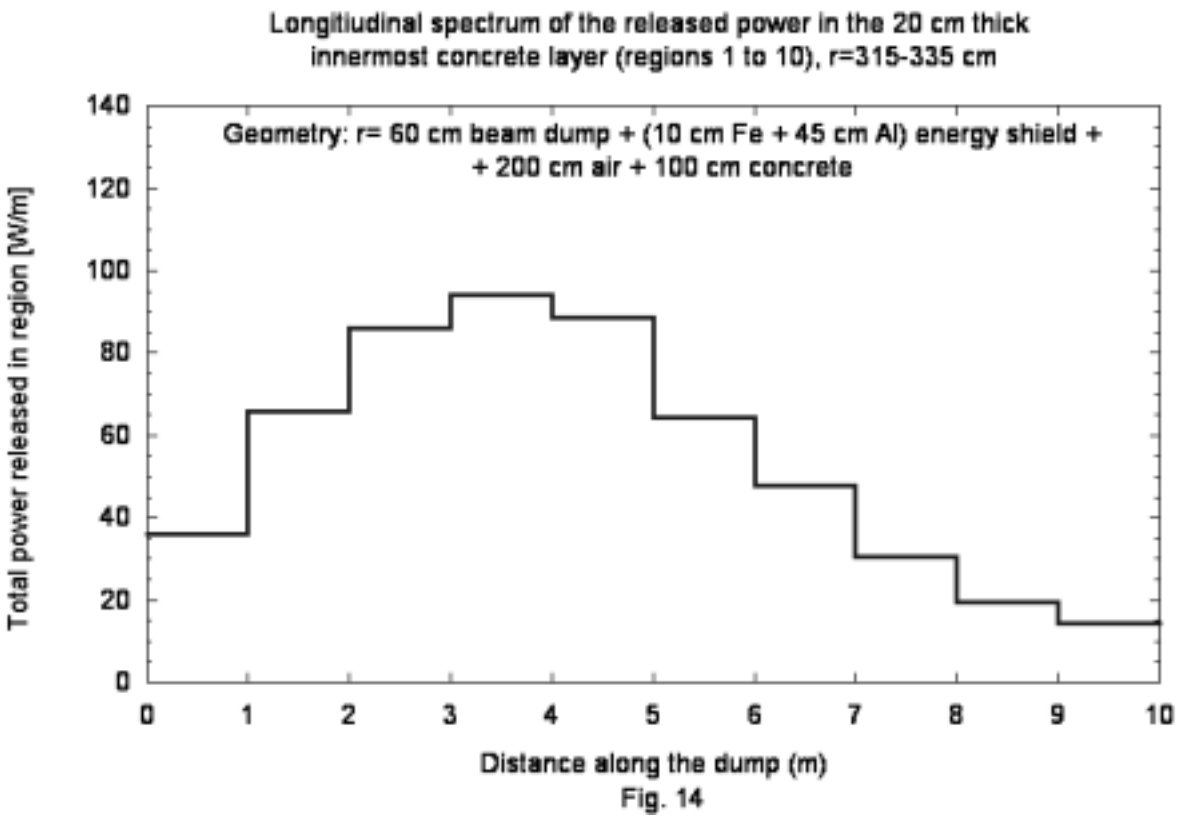
Longitiudinal spectrum of the released power in the 20 cm thick
innermost concrete layer (regions 1 to 10), r=315-335 cm
Geometry: r= 60 cm beam dump + (10 cm Fe + 45 cm Al) energy shield +
+ 200 cm air + 100 cm concrete
Total power released in region [W/m]
Distance along the dump (m)
0
20
40
60
80
100
120
140
0
1
2
3
4
5
6
7
8
9
10
Fig. 14

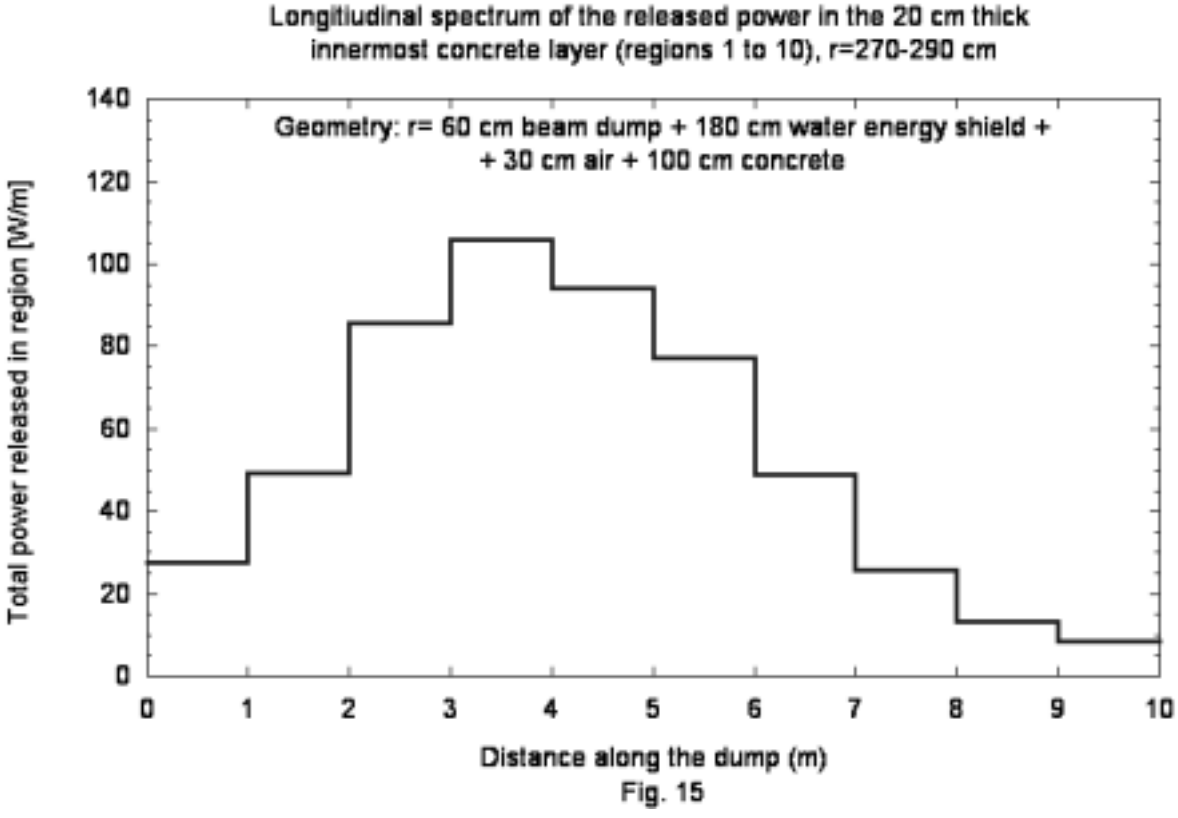
Longitiudinal spectrum of the released power in the 20 cm thick
innermost concrete layer (regions 1 to 10), r=270-290 cm
Geometry: r= 60 cm beam dump + 180 cm water energy shield +
+ 30 cm air + 100 cm concrete
Total power released in region [W/m]
Distance along the dump (m)
0
20
40
60
80
100
120
140
0
1
2
3
4
5
6
7
8
9
10
Fig. 15